

2008

## Suction Generation in White-Spotted Bamboo Sharks *Chiloscyllium Plagiosum*

Cheryl D. Wilga  
*University of Rhode Island, cwilga@uri.edu*

Christopher P. Sanford

Follow this and additional works at: [https://digitalcommons.uri.edu/bio\\_facpubs](https://digitalcommons.uri.edu/bio_facpubs)

Terms of Use

All rights reserved under copyright.

---

### Citation/Publisher Attribution

Wilga, C.D. and C.P. Sanford. 2008. Suction generation in white-spotted bamboo sharks *Chiloscyllium plagiosum*. *Journal of Experimental Biology*. 211:3128-3138. Available at doi:10.1242/jeb.018002

This Article is brought to you for free and open access by the Biological Sciences at DigitalCommons@URI. It has been accepted for inclusion in Biological Sciences Faculty Publications by an authorized administrator of DigitalCommons@URI. For more information, please contact [digitalcommons-group@uri.edu](mailto:digitalcommons-group@uri.edu).

---

## Suction Generation in White-Spotted Bamboo Sharks *Chiloscyllium Plagiosum*

Terms of Use

All rights reserved under copyright.

## Suction generation in white-spotted bamboo sharks *Chiloscyllium plagiosum*

Cheryl D. Wilga<sup>1,\*</sup> and Christopher P. Sanford<sup>2</sup>

<sup>1</sup>Department of Biological Sciences, University of Rhode Island, Kingston, RI 02881, USA and <sup>2</sup>Department of Biology, 114 Hofstra University, Hempstead, NY 11549, USA

\*Author for correspondence (e-mail: cwilga@uri.edu)

Accepted 14 July 2008

### SUMMARY

After the divergence of chondrichthyans and teleostomes, the structure of the feeding apparatus also diverged leading to alterations in the suction mechanism. In this study we investigated the mechanism for suction generation during feeding in white-spotted bamboo sharks, *Chiloscyllium plagiosum* and compared it with that in teleosts. The internal movement of cranial elements and pressure in the buccal, hyoid and pharyngeal cavities that are directly responsible for suction generation was quantified using sonomicrometry and pressure transducers. Backward stepwise multiple linear regressions were used to explore the relationship between expansion and pressure, accounting for 60–96% of the variation in pressure among capture events. The progression of anterior to posterior expansion in the buccal, hyoid and pharyngeal cavities is accompanied by the sequential onset of subambient pressure in these cavities as prey is drawn into the mouth. Gape opening triggers the onset of subambient pressure in the oropharyngeal cavities. Peak gape area coincides with peak subambient buccal pressure. Increased velocity of hyoid area expansion is primarily responsible for generating peak subambient pressure in the buccal and hyoid regions. Pharyngeal expansion appears to function as a sink to receive water influx from the mouth, much like that of compensatory suction in bidirectional aquatic feeders. Interestingly, *C. plagiosum* generates large suction pressures while paradoxically compressing the buccal cavity laterally, delaying the time to peak pressure. This represents a fundamental difference from the mechanism used to generate suction in teleost fishes. Interestingly, pressure in the three cavities peaks in the posterior to anterior direction. The complex shape changes that the buccal cavity undergoes indicate that, as in teleosts, unsteady flow predominates during suction feeding. Several kinematic variables function together, with great variation over long gape cycles to generate the low subambient pressures used by *C. plagiosum* to capture prey.

Key words: suction feeding, biomechanics, shark, sonomicrometry.

### INTRODUCTION

Suction feeding is by far the most common means by which aquatic vertebrates capture prey (Lauder, 1985; Lauder and Shaffer, 1993; Ferry-Graham and Lauder, 2001; Motta and Wilga, 2001; Motta, 2004). Rapid expansion of the mouth and hyoid cavities generates the rapid pressure drop in the buccal cavity that draws water and prey into the mouth of a suction-feeding fish (Liem, 1978; Liem, 1980; Lauder, 1980a; Lauder, 1980b; Lauder, 1983; Van Leeuwen and Muller, 1983; Muller and Osse, 1984; Lauder et al., 1986; Sanford and Wainwright, 2002; Svanbäck et al., 2002). An anterior to posterior progression of gape, hyoid and branchial expansion occurs during suction capture of prey (Liem, 1980; Lauder, 1985; Lauder and Shaffer, 1993; Wilga and Motta, 1998a; Wilga and Motta, 1998b). This progression of expansion functions to move water and prey through the cavities of the head towards the esophagus (Lauder, 1985; Liem, 1980; Wilga and Motta, 1998a; Wilga and Motta, 1998b; Sanford and Wainwright, 2002). Only two studies have measured internal kinematics simultaneously with intraoral pressure recordings to investigate suction feeding in largemouth bass (Sanford and Wainwright, 2002; Carroll and Wainwright, 2006). In those studies, peak gape pressure was found to coincide with the time of peak rate of percentage change in hyoid area (Sanford and Wainwright, 2002). Furthermore, kinematics using internal sonometric data was able to account for considerably more of the variation (90–99%) among suction-feeding events (Sanford and Wainwright, 2002) than that using external video recordings (<55%) (Svanbäck et al., 2002).

The structure and function of the feeding apparatus diverged considerably after the split between chondrichthyan and teleostome fishes (Lauder and Shaffer, 1993; Wilga et al., 2000; Wilga, 2002; Westneat, 2006; Wilga, 2008). The head skeleton of elasmobranchs is relatively simple compared with that of actinopterygians due to the fewer number of cranial elements representing fewer degrees of freedom. The hyoid arch is composed of hyomandibular, ceratohyal and basihyal cartilages while that of teleosts has several additional dermal bones interconnecting the hyomandibula and ceratohyal cartilages (Wilga, 2002). The decreased number of musculoskeletal elements and degrees of freedom has been shown to limit hyoid kinetics in some sharks compared with that in actinopterygians (Wilga, 2008). In both groups, the hyoid depresses ventrally during suction feeding, thus expanding hyoid volume (Lauder and Shaffer, 1993; Sanford and Wainwright, 2002; Westneat, 2006). In actinopterygians, the hyoid is ventrally directed from the cranium and also expands laterally during suction feeding (Lauder and Shaffer, 1993; Sanford and Wainwright, 2002; Westneat, 2006). However, in shark species with laterally directed hyomandibulae, the lateral width of the hyoid (between hyomandibular tips) becomes smaller during feeding (Wilga, 2008). In these shark species the distal tips of the hyomandibulae are already maximally distant at rest and are constrained to adduct and therefore move ventrally when the basihyal is depressed, causing the inter-tip distance to decrease (Wilga, 2008). How this disparity in hyomandibular morphology between actinopterygians and sharks affects the generation of suction feeding is of great interest since

hyoid movement is a key component in the suction-feeding mechanism of actinopterygians (Lauder and Shaffer, 1993; Westneat, 2006).

The mechanism for lower jaw depression also differs between chondrichthyans and actinopterygians (Wilga et al., 2000). Chondrichthyans have one muscular linkage between the pectoral girdle and lower jaw to depress the lower jaw and another linkage between the pectoral girdle and basihyal that depresses the hyoid. These muscles have been replaced by other muscles in actinopterygians, resulting in a linkage whereby depression of the hyoid also depresses the lower jaw (Lauder and Shaffer, 1993; Wilga et al., 2000; Van Wassenbergh et al., 2005). In essence, chondrichthyans have independent parallel mechanisms for depressing the lower jaw and hyoid, while actinopterygians have a linked in-series mechanism for depressing the hyoid and lower jaw simultaneously (Wilga et al., 2000). This disparity in jaw depression in chondrichthyans may affect the generation of suction feeding compared with that in teleosts.

The functional separation of pharyngeal and parabranial cavities differs between chondrichthyans and actinopterygians. In elasmobranchs, the pharyngeal cavity contains at least five branchial arches with parabranial cavities that are functionally continuous (Summers and Ferry-Graham, 2001) and lie posterior to the cranium. In contrast, the branchial arches lie ventral to the cranium with a well-defined opercular cavity that is functionally separate in bony fishes (Lauder, 1983; Lauder, 1984). Whether pharyngeal expansion assists buccal expansion in generating suction pressure to capture prey has not yet been determined. These fundamental morphological distinctions between chondrichthyans and actinopterygians may alter details of the suction mechanism, yet yield similar results, i.e. prey capture by suction. How the suction mechanism has been altered after the evolutionary divergence between chondrichthyans and actinopterygians is of great interest to functional and evolutionary biologists.

In this study, we investigated how white-spotted bamboo sharks, *Chiloscyllium plagiosum*, which have laterally directed hyomandibulae, generate intraoral suction pressure to capture prey and evaluated whether the mechanism for generating that suction has diverged between chondrichthyans and actinopterygians. We measured internal expansion and pressure generation in the buccal, hyoid and pharyngeal cavities using sonomicrometry and internal pressure probes. More specifically, we asked the following questions that test previous hypotheses regarding suction feeding in fishes. (1) Does the progression of maximum subambient pressure during suction feeding in *C. plagiosum* parallel the progression of kinematic expansion? (2) Does the time of peak area change coincide with the time of maximum suction pressure in the three regions during suction feeding in *C. plagiosum*? (3) Is the temporal relationship between expansion of the buccal cavity and the resulting subambient pressure generated in *C. plagiosum* similar to that of teleosts? (4) Does the morphological constraint in hyomandibular function causing adduction in sharks during feeding impede the generation of suction? (5) Does pharyngeal expansion directly contribute to suction generation that assists in capturing prey?

## MATERIALS AND METHODS

### Animals

White-spotted bamboo sharks *Chiloscyllium plagiosum* (Bennett 1830) were obtained from SeaWorld of San Diego, CA, USA. The sharks were housed together in a 3028 l circular tank at 24.4°C with a 12 h–12 h light:dark cycle and maintained on a diet of squid (*Loligo* sp.) and fish (Atlantic silversides, *Menidia menidia*). Four

individuals were used with total lengths of 69, 71, 74 and 76 cm. An individual shark was placed in a 757 l circular experimental tank to acclimate for 3 days with food withheld. The fish was anesthetized for surgery with a 0.1 g l<sup>-1</sup> solution of tricaine methanesulfonate (MS-222), which was diluted to 0.05 g l<sup>-1</sup> during implantation of the sonometric crystals and pressure transducers. After surgery, the fish was allowed to recover in the experimental tank for up to 4 h before feeding behavior was recorded. Pieces of squid cut into one mouth width (mw) × 1/2 mw size were fed to the fish until satiation. Due to the large number of crystals implanted, two experimental protocols were run on each individual, one protocol on gape and hyoid expansion and the second on gape and pharyngeal expansion.

### Sonomicrometry

The kinematics of 13 internal locations on the walls of the buccal, hyoid and pharyngeal cavities was measured using sonometric crystals (Fig. 1). Gape distance was transduced using crystals 2 and 3. Upper jaw protrusion was transduced using crystals 1 and 2. Gape area was calculated based on an expanding circle, verified by video recordings, using gape distance. Hyoid lateral width (expansion) was transduced from crystals 5 and 6. Hyoid vertical depression was calculated by using the law of cosines to calculate a vertical distance between crystal 7 and a line formed by crystals 1 and 4. The law of cosines required transducing distances between crystals 7 and 1, 7 and 4, and 1 and 4 (for details, see Sanford and Wainwright, 2002). Hyoid area was calculated based on an expanding ellipse using hyoid vertical depression and lateral width expansion. Pharyngeal lateral width (expansion) was transduced from crystals 9 and 10. Pharyngeal vertical depression was calculated in a similar way to hyoid depression using the law of cosines to calculate a vertical distance between crystal 11 and a line formed by crystals 12 and 13. The law of cosines required transducing distances between crystals 11 and 12, 11 and 13, and 12 and 13. Pharyngeal area was calculated based on an expanding ellipse using pharyngeal vertical depression and lateral width. Gape, hyoid and pharyngeal expansion could not be quantified simultaneously due to the large number of wires and pressure probes that would have filled the orobranchial cavity; therefore, gape expansion served as the reference and was measured with either hyoid or pharyngeal expansion, and thus pharyngeal volume could not be calculated.

The crystals used were 2 mm diameter omnidirectional piezoelectric crystals with two suture loops on opposite sides of the crystal perpendicular to the wire (Sonometrics, Ontario, Canada). Both loops were sutured to the skin at each location. The wires from the crystals were separated into two bundles, threaded out through each fifth gill slit and sutured to the skin anterior to the first dorsal fin. The fifth gill slit remains open during most of the feeding cycle (Dolce and Wilga, 2005). The sharks did not appear to be bothered by the wires running through the fifth gill slit; they ate readily and ventilated normally during the experiments.

The kinematics of gape–hyoid and gape–pharyngeal expansion was recorded using a 16 channel digital sonomicrometer (Sonometrics) with resolution enhancement to 0.015 mm. SonoVIEW software (Sonometrics) was used to record sonometric data of feeding sharks at a sampling rate of 409.16 Hz and transmit pulse of 250 ns with an inhibit delay of 3.44 μs and 4.57 mm. The distance between selected pairs of crystals was transduced in SonoVIEW and exported to SigmaPlot (Jandel, CA, USA) for graphing; Excel (Microsoft, WA, USA) was used to calculate the variables not directly transduced. Plots *versus* time were used to derive temporal, displacement and velocity variables for each feeding sequence. Temporal variables included time of onset, and

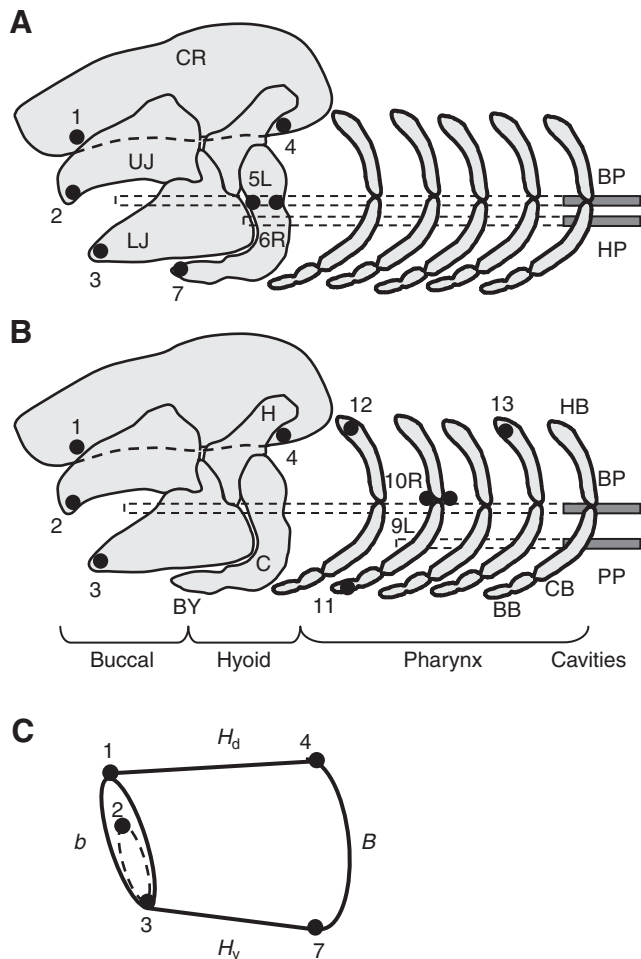


Fig. 1. Location of sonometric crystals (black circles) and pressure probes (gray bars, sensor location at dashed end of bars) for (A) gape and hyoid and (B) gape and pharyngeal experiments. (C) Conical frustum model.  $B$ , posterior buccal surface area;  $b$ , anterior buccal surface area; BY, basihyal; BB, basibranchial; BP, buccal pressure probe; C, ceratohyal; CR, cranium; H, hyomandibula;  $H_d$ , dorsal buccal length;  $H_v$ , ventral buccal length; HB, epibranchial; HP, hyoid pressure probe; L, left; LJ, lower jaw; PP, pharyngeal probe; R, right; UJ, upper jaw. Dotted circle in C represents gape area.

duration to and time of peak for gape, hyoid and pharyngeal area. *Chiloscyllium plagiosum* is a suction ventilator, thus there are continuous cycles of subambient to superambient pressures in the buccal, hyoid, pharyngeal and parabranchial cavities and small opening and closing cycles of the mouth that a feeding sequence interrupts. As a result, the time at which 10% of peak gape height was attained was defined as the time of onset of gape area (Sanford and Wainwright, 2002). The time of peak suction pressure in the buccal cavity was set as time zero ( $t_0$ ) for reference to other variables. Displacement variables calculated included peak area and change in area for gape, hyoid and pharyngeal area and buccal volume. Velocity variables calculated included time of peak and peak velocity, and time of peak and peak rate of percentage change in gape, hyoid and pharyngeal area.

Buccal volume using the volume of a conical frustum was calculated for each feeding event using sonometric crystals (Fig. 1C). A conical frustum, or a truncated cone, with a parallel base and top roughly resembles the shape of the buccal cavity of a bamboo shark. Thus, the equation for the volume of a conical frustum,

$V=(H/3)\times(B+b+\sqrt{Bb})$ , was used to estimate the volume of the buccal cavity, where  $H$  is the height of the cone, and  $B$  and  $b$  are parallel areas of opposite ends of the cone. In this model, the cone rests on one side with  $H$  representing the length of the buccal cavity,  $B$  is the base representing the cross-sectional area at the hyoid arch, and  $b$  is the truncated cross-sectional top area at the mouth end. However, the ventral length of the buccal cavity is shorter than the dorsal length of the buccal cavity, particularly at peak gape when the lower jaw and basihyal have rotated posteroventrally. The volume based on using the dorsal length of the buccal cavity  $H_d$ , represented by crystals 1 to 4, is an overestimate of buccal cavity volume at peak gape due to the posteroventral movement of the lower jaw. Similarly, the volume based on using the ventral length of the buccal cavity  $H_v$ , represented by crystals 3 to 7, is an underestimate of buccal cavity volume at peak gape because the anterior cranial volume is not included. Since the lower jaw swings in an even arch, a better estimate of buccal volume used here was calculated by taking the mean of both volumes. Areas  $B$  and  $b$  remain the same in the two calculations. Area  $B$  is peak hyoid area calculated as above by transducing the vertical height from crystals 1, 4 and 7. Area  $b$  is the anterior mouth end described by peak gape width (crystals 2 to 3) multiplied by the distance from the anterior cranium to the lower jaw (crystals 1 to 3).

### Pressure

Pressure was recorded simultaneously with sonomicrometry using two Millar SPR-799 microcatheter side-tipped pressure transducers. The pressure probes were threaded through a plastic cannula, then inserted through the fifth gill slit and fixed to the skin by suture. One probe was sutured on the midline buccal cavity roof just behind the teeth while the second was sutured to the midline of the roof either between the hyomandibulae or between the second gill arches. The pressure probes were connected to an analog channel on the sonomicrometry system for precise synchronization of pressure and kinematic data. Pressure recordings were analyzed using SonoVIEW for the following pressure variables relative to ambient for buccal, hyoid and pharyngeal cavities: time of onset, duration from onset to peak, time of peak, peak magnitude, peak rate of change, and time of peak rate of change of subambient pressure.

### Statistical analysis

Multiple stepwise linear regressions were used as an exploratory tool to find relationships between pressure and gape, hyoid and pharyngeal area changes. Two sets of analyses were run for each of the areas, one using the onset of pressure and one using peak pressure (kPa) as the dependent variable and 10 gape and hyoid or gape and pharyngeal kinematic variables as the independent variables: time of onset of buccal and hyoid-pharyngeal expansion, time of peak buccal and hyoid-pharyngeal pressure, peak buccal and hyoid-pharyngeal area ( $\text{mm}^2$ ), the rate of change in gape and hyoid-pharyngeal area ( $\text{mm}^2\text{ms}^{-1}$ ) and time of peak rate of change in buccal and hyoid-pharyngeal expansion area. We removed variables that could be derived from other variables to eliminate autocorrelation. All of the variables with  $P$ -values greater than 0.3 (to be conservative) were removed. Each analysis was run in a stepwise manner. In the reduced model all of the variables with  $P$ -values greater than 0.3 were removed. This step was rerun until all  $P$ -values were less than 0.3, which are the models presented here. Standardized estimates as well as  $r^2$  values are reported to indicate the explanatory power that each variable contributes to the reduced model. Standard estimates indicate the magnitude and direction of a change incurred while  $r^2$  values provide the magnitude of

covariation. Individuals were included as a categorical variable. Interaction effects were not included for clarity.

A mixed model two-way analysis of variance (ANOVA) was used to test pressure and area variables among gape, buccal, hyoid and pharyngeal regions. Individual is a random main effect, and region is a fixed main effect tested by the individual $\times$ region term. If a difference was detected by ANOVA, a Tukey's Studentized range test was applied. Several paired *t*-tests were performed to determine which kinematic variables may be responsible for pressure variables; the reference time (0 ms) was set at the time of peak gape pressure. Linear regressions were used to evaluate the contribution of buccal volume to suction generation. Statistical tests were calculated using SAS (v.8.1; Cary, NC, USA) or SigmaStat (v.3.1; San Jose, CA, USA). Buccal variables were combined from hyoid and pharyngeal experiments; *N*=4, 10 feeding events per individual. Hyoid and pharyngeal variables were from hyoid or pharyngeal experiments; *N*=4, five feeding events per individual per protocol. The same individuals were used in the two protocols for a total of 40 feeding events.

## RESULTS

All of the shark individuals used suction to capture squid as has been found previously (Nauwelaerts et al., 2007). An anterior to posterior progression of expansion begins in the gape and hyoid cavities followed by the pharyngeal cavity (Fig. 2; Table 1). The onset of pressure in the buccal, hyoid and pharyngeal cavities begins immediately after the mouth opens. The gape attains peak expansion just prior to peak buccal pressure. The hyoid and pharyngeal cavities continue to expand until well after peak buccal pressure and peak simultaneously. Hyoid expansion is greater than pharyngeal expansion, which is greater than that of the gape (Table 2). Peak rate of change in area is greater in the hyoid than in the gape and pharynx. The time of peak rate of change occurs later in the pharyngeal cavity than in the gape and hyoid cavities.

A representative raw sonometric and pressure trace of a gape–hyoid suction feeding event shows that lower jaw and hyoid movements occur as pressure in the buccal and hyoid regions rapidly decreases (Fig. 3; Table 1). Lower jaw and hyoid depression are simultaneous with a subambient pressure decrease in the buccal and hyoid regions. As the basihyal is depressed ventrally, the distal ends of the hyomandibulae move closer together medially. Inflection points where hyoid pressure drop stalls momentarily occur as hyoid width begins to decrease laterally and then again as hyoid width increases laterally. The basihyal moves posteroventrally in an arc during the expansive phase of suction feeding (Fig. 4A). Peak posterior movement of the basihyal occurs after peak subambient hyoid pressure and coincides with minimum hyoid lateral width. Hyoid vertical depression occurs early and rapidly, while hyoid lateral width does not begin to decrease until about 20 ms later (Fig. 3; Fig. 4B). Due to the shape of the hyoid cavity, the lateral span is larger than the vertical span, even at peak hyoid area expansion.

A representative raw sonometric and pressure trace of a gape–pharyngeal suction-feeding event shows that lower jaw and pharyngeal depression movements are greater in magnitude than lateral pharyngeal movements as pressure in the buccal and hyoid regions drops (Fig. 5). In contrast to hyoid movements, pharyngeal vertical depth and lateral width increase and decrease synchronously during suction feeding. Note that peak subambient pressure in the pharyngeal region occurs well before peak pharyngeal depression.

Representative plots of gape and hyoid area and buccal and hyoid pressure from sonometric and pressure data illustrate a gape–hyoid

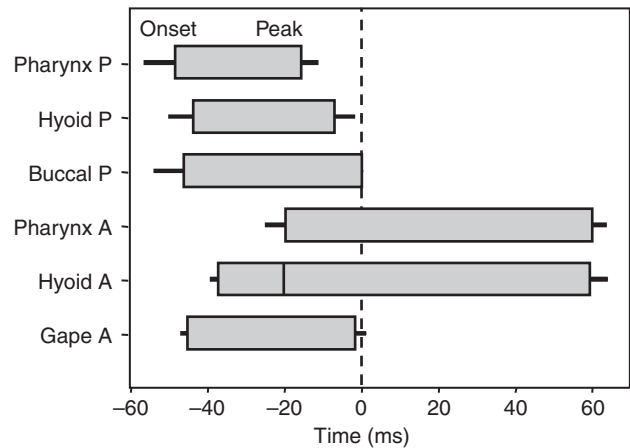


Fig. 2. Bar plot showing mean onset and peak times with s.e.m. bars in selected area (A) and pressure (P) variables during suction feeding in *Chiloscyllium plagiosum*. *N*=4, 10 feeding events per individual. Vertical bar at -20 ms on hyoid area bar indicates the point at which hyoid lateral width begins to decrease.

suction-feeding event (Fig. 6). Subambient pressure in the buccal and hyoid cavities decreases rapidly and synchronously during expansion of the gape and hyoid cavities in strong feeding events. Peak buccal and hyoid pressures are reached as early as 27 and 22 ms, respectively, after the onset of subambient pressure drop, with a mean of 48 and 37 ms, respectively. Pressure in the cavities returns to ambient relatively rapidly as the gape is reduced to closing. In contrast, hyoid expansion reaches a plateau and slowly decreases back to the resting position. Representative plots of gape and pharyngeal area and buccal and pharyngeal pressure from sonometric and pressure data illustrate a gape–pharyngeal suction-feeding event (Fig. 7; Table 1). A small decrease in pharyngeal area occurs immediately prior to the subambient pressure drop, indicating that a preparatory phase may be present. Pressure in the pharynx begins to drop at a mean of 3.6 ms prior to pharyngeal expansion.

Linear regression plots show a weak, but nevertheless significant, relationship between several variables during suction feeding (Fig. 8). Buccal volume contributes little to the variation in time to peak area in the gape ( $r^2=0.13$ ,  $P<0.001$ ) and hyoid ( $r^2=0.07$ ,  $P<0.001$ ) regions. Buccal volume also contributes little to the variation in buccal ( $r^2=0.16$ ,  $P=0.001$ ) and hyoid ( $r^2=0.14$ ,  $P=0.002$ ) pressure. Multiple regression models recovered kinematic variables that account for 77% of the variation in the onset of buccal pressure, 60% of the variation in peak buccal pressure, 74% of the variation in the onset of hyoid pressure and 63% of the variation in peak hyoid pressure in the gape–hyoid events (Tables 3–6). The models recovered kinematic variables accounting for 96% of the variation in the onset of pharyngeal pressure and 81% of the variation in peak pharyngeal pressure in the gape–pharyngeal events (Tables 7 and 8). The only variable with an individual effect is time of peak pharyngeal area expansion ( $P=0.001$ , individual 4 differs from 1, 2 and 3); however, this variable was not a major factor in any of the analyses.

The onset of subambient pressure is similar in the three cavities and is coincident with the onset of gape opening (Table 2). However, subambient pressure peaks first in the pharynx, then hyoid and lastly in the buccal cavity. The magnitude of peak subambient pressure is similar in the buccal and hyoid cavities and larger than that in the pharynx. The mean rate of pressure drop is similar in the buccal, hyoid and pharyngeal cavities. The time of pressure peak velocity occurs earlier in the hyoid and pharyngeal cavities than that in the

Table 1. Summary means of pressure and sonometric variables during suction feeding in *Chiloscyllium plagiosum*

Variables	Mean	s.e.m.	Maximum	Minimum
<b>Pressure (subambient)</b>				
Buccal pressure, onset (ms)	-47.94	5.53	-26.88	-76.70
Buccal pressure, peak (kPa)	-20.58	5.97	-5.87	-45.46
Buccal pressure, peak rate of change (kPa ms <sup>-1</sup> )	-1.40	0.51	-0.20	-4.53
Buccal pressure, peak rate of change (ms)	-8.38	5.7	0.00	-37.62
Hyoid pressure, onset (ms)	-43.91	4.15	-30.10	-60.19
Hyoid pressure, peak (ms)	-7.10	7.12	7.66	-30.10
Hyoid pressure, peak (kPa)	-22.39	2.63	-8.87	-42.46
Hyoid pressure, duration to peak (ms)	36.82	5.63	22.57	60.19
Hyoid pressure, peak rate of change (kPa ms <sup>-1</sup> )	-1.42	0.48	-0.31	-4.55
Hyoid pressure, peak rate of change (ms)	-20.18	5.44	3.65	-37.62
Pharynx pressure, onset (ms)	-46.07	5.95	-24.44	-58.66
Pharynx pressure, peak (ms)	-16.22	5.78	2.44	-36.82
Pharynx pressure, peak (kPa)	-11.39	2.60	-4.93	-21.00
Pharynx pressure, duration to peak (ms)	32.83	5.08	61.10	19.55
Pharynx pressure, peak rate of change (kPa ms <sup>-1</sup> )	-0.75	0.24	-0.26	-2.10
Pharynx pressure, peak rate of change (ms)	-26.78	6.54	-2.44	-42.95
<b>Kinematic</b>				
Gape area, onset (ms)	-45.20	5.21	-22.00	-67.72
Gape area, peak (ms)	-1.65	8.0	33.75	-31.77
Gape area, peak duration (ms)	42.85	7.94	73.63	15.34
Gape area, peak (mm <sup>2</sup> )	206.28	24.67	351.50	133.10
Gape area, peak rate of change (mm <sup>2</sup> ms <sup>-1</sup> )	9.23	1.56	18.85	3.30
Gape area, peak rate of change (ms)	-26.01	2.8501	7.72	-55.22
Gape area, peak rate of percentage change (%)	9.50	2.23	26.49	4.86
Gape area, peak rate of percentage change (ms)	-30.43	6.20	-9.20	-55.22
Gape area, change (mm <sup>2</sup> )	155.13	22.48	288.24	62.90
Hyoid area, onset (ms)	-37.40	3.82	-22.57	-45.94
Hyoid area, peak (ms)	59.30	9.60	82.76	22.97
Hyoid area, peak duration (ms)	96.12	10.39	127.91	52.67
Hyoid area, peak (mm <sup>2</sup> )	510.17	33.85	672.33	386.74
Hyoid area, peak rate of change (mm <sup>2</sup> ms <sup>-1</sup> )	17.38	4.42	44.02	8.57
Hyoid area, peak rate of change (ms)	-19.22	4.00	0.00	-38.28
Hyoid area, peak rate of percentage change (%)	15.88	7.63	52.88	2.62
Hyoid area, peak rate of percentage change (ms)	-24.12	4.48	0.00	-38.28
Hyoid area, change (mm <sup>2</sup> )	379.74	46.79	592.97	218.65
Pharynx area, onset (ms)	-19.78	6.95	4.89	-51.32
Pharynx area, peak (ms)	59.85	12.09	116.58	17.11
Pharynx area, peak duration (ms)	79.63	13.06	138.06	43.99
Pharynx area, peak (mm <sup>2</sup> )	396.69	56.11	632.35	230.67
Pharynx area, peak rate of change (mm <sup>2</sup> ms <sup>-1</sup> )	11.11	2.48	5.00	25.88
Pharynx area, peak rate of change (ms)	2.22	9.11	41.55	-36.66
Pharynx area, peak rate of percentage change (%)	7.65	4.23	40.52	1.92
Pharynx area, peak rate of percentage change (ms)	-1.39	9.10	41.55	-36.66
Pharynx area, change (mm <sup>2</sup> )	258.46	46.42	492.36	116.30

Times are relative to  $t_0$ =time of peak buccal pressure. Buccal variables are from hyoid and pharyngeal experiments;  $N=4$ , 10 feeding events per individual. Hyoid and pharyngeal variables are from hyoid or pharyngeal experiments;  $N=4$ , five feeding events per individual per protocol.

buccal cavity. Several paired  $t$ -tests were run with a Bonferroni correction of  $P=0.005$ . The peak in buccal pressure occurs at the same time as peak gape opening ( $P=0.517$ ). The onset of buccal pressure occurs at the same time as the onset of gape opening ( $P=0.419$ ). The onset of hyoid pressure occurs at the same time as the onset of hyoid expansion ( $P=0.006$ ). The onset of pharyngeal pressure occurs prior to the onset of pharyngeal expansion ( $P<0.001$ ). The time of peak rate of change (velocity) in gape area occurs earlier than the time of peak gape pressure ( $P<0.001$ ). The time of peak percentage velocity in gape area occurs earlier than the time of peak gape pressure ( $P<0.001$ ). The peak velocity in the hyoid area occurs at the same time as peak hyoid pressure ( $P=0.005$ ). The time of peak percentage velocity in the hyoid area occurs earlier than the time of peak hyoid pressure ( $P<0.001$ ). The peak pharyngeal pressure occurs at the same time as the peak velocity and the peak percentage velocity in the pharyngeal area ( $P<0.006$  and  $P=0.012$ ).

## DISCUSSION

*Chiloscyllium plagiosum* rapidly expands the buccal and hyoid cavities using powerful hypertrophied hypobranchial muscles (Ramsay and Wilga, 2007), enabling rapid fluid inflow into the mouth when suction feeding, as in other aquatic suction-feeding vertebrates. Interestingly, *C. plagiosum* generates large suction pressure while paradoxically compressing the buccal cavity laterally. The complex shape changes that the buccal cavity undergoes during a suction event indicate that, as in teleosts, unsteady flow predominates during a suction event (Higham et al., 2006). The progression of anterior to posterior expansion in the buccal, hyoid and pharyngeal cavities is accompanied by the sequential onset of subambient pressure in those cavities as prey is drawn into the mouth by suction. This conserved pattern exists even in taxa that are considered to be bite feeders, which also sequentially expand the buccal, hyoid and pharyngeal cavities, albeit less rapidly (Wilga

Table 2. Results of two-way ANOVA on pressure and kinematic variables among gape, buccal, hyoid and pharyngeal regions during suction feeding in *C. plagiosum*

Variables	F-ratio	P-value	Tukey MCT
Pressure onset (ms)	0.98	0.3790	
Pressure peak subambient (kPa)	9.49	0.0002	BH<P
Pressure peak (ms)	51.11	<0.0001	P<H<B
Pressure duration subambient (ms)	12.77	<0.0001	B<HP
Pressure peak velocity (kPa ms <sup>-1</sup> )	4.51	0.0145	
Pressure peak velocity (ms)	20.74	0.0001	B<HP
Area onset (ms)	35.83	<0.0001	GH<P
Area peak (ms)	42.92	<0.0001	G<HP
Area peak duration (ms)	65.95	<0.0001	G<P<H
Area peak (mm <sup>2</sup> )	59.55	<0.0001	G<P<H
Area peak change (mm <sup>2</sup> )	69.07	<0.0001	G<P<H
Area peak change rate (mm <sup>2</sup> ms <sup>-1</sup> )	15.48	<0.0001	GP<H
Area peak change rate (ms)	39.92	<0.0001	GH<P

B, buccal; G, gape; H, hyoid; P, pharyngeal. Bonferroni *P*-value is 0.0038. MCT, multiple comparison test.

and Motta, 2000; Motta and Wilga, 2001; Motta, 2004), to provide adequate space for the prey to enter the oropharyngeal cavity. Thus, the pattern may be ubiquitous and does not appear to limit the range of feeding strategies utilized in fishes. Interestingly, pressure in the three cavities peaks in the posterior to anterior direction. The pharynx functions as a sink to accumulate water influx from the buccal cavity rather than directly generating suction to assist in prey capture. Multiple stepwise linear regressions based on internal kinematics account for 60–96% of the variation in onset and peak pressure among suction capture events, similar to the 61–74% variation detected in *Micropterus salmoides* (excluding individual and interaction effects) (Sanford and Wainwright, 2002). The relationship between kinematics and pressure appears to be tightly integrated. Several kinematic variables function together, each contributing to the variation in pressure over relatively long gape cycles, compared with teleosts, to generate the very low subambient pressures used by *C. plagiosum* to capture prey.

#### Factors driving the onset of buccal and hyoid pressure

The onset of pressure in the buccal and hyoid cavities occurs simultaneously indicating that the two regions are not functionally

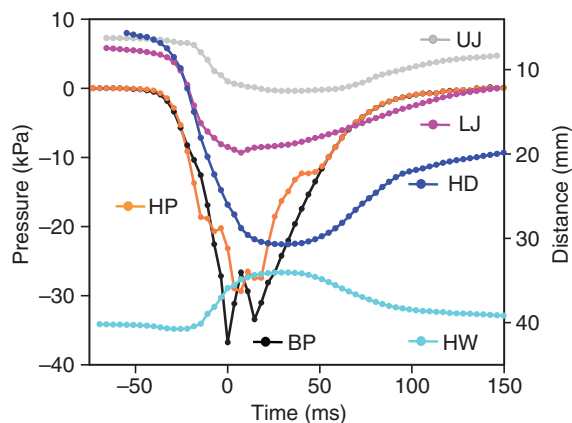


Fig. 3. Representative plot of buccal and hyoid kinematic and pressure variables during a suction-feeding event in *Chiloscyllium plagiosum*. Kinematic traces: HD, hyoid depression, blue; HW, hyoid lateral expansion, light blue; LJ, lower jaw depression, pink; UJ, upper jaw protrusion, gray. Pressure traces: BP, buccal pressure, black; HP, hyoid pressure, orange.

distinct during the initial phase of suction generation. It is primarily the onset of gape area increase that triggers the onset of subambient pressure in the buccal and hyoid cavities during suction feeding in *Chiloscyllium plagiosum* (Fig. 8). The onset of buccal and hyoid pressure occurs simultaneously with the onset of mouth opening and hyoid expansion. The onset of hyoid expansion also assists the gape in initiating the subambient pressure drop in the buccal cavity. Mouth opening allows water to be drawn in by the subambient pressure gradient as the hyoid simultaneously begins to expand: a finding originally suggested by Van Leeuwen (Van Leeuwen, 1984). Indeed, subambient pressure drops rapidly as the mouth opens during suction feeding in teleosts as well (Lauder, 1980b; Sanford and Wainwright, 2002). In contrast, the onset of subambient pressure in the buccal cavity more closely corresponds with the onset of hyoid depression in *Micropterus salmoides* (Sanford and Wainwright, 2002). The same kinematic variables account for 66% and 59% of the variation in the onset of pressure in the buccal and hyoid regions, with the same variables contributing similar proportions. The onset of gape and hyoid area and peak velocity of gape and hyoid area contribute the most to variation in the onset of subambient pressure in the buccal and hyoid cavities. An earlier onset of gape opening and the faster rate

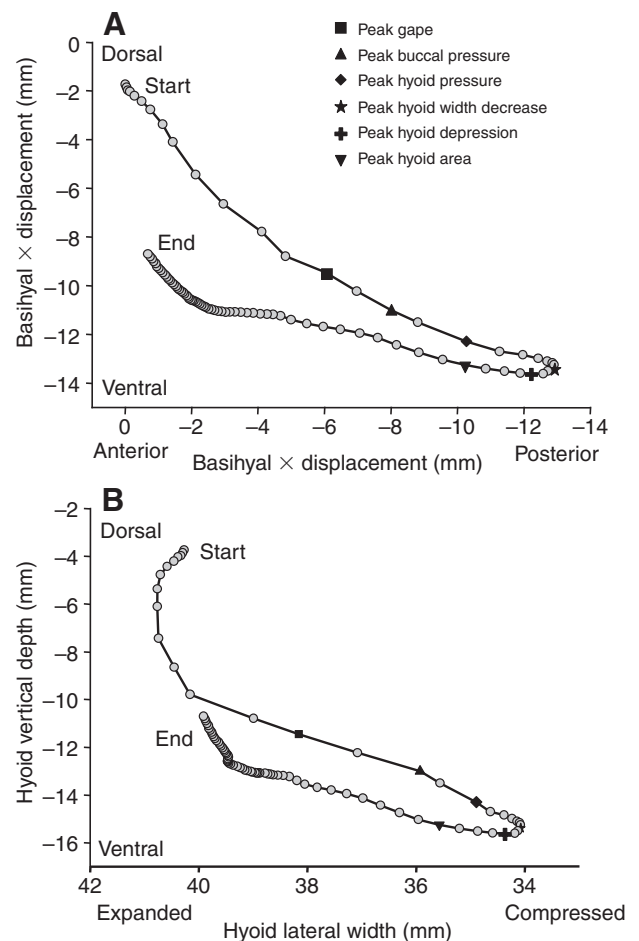


Fig. 4. Representative plot of hyoid movement relative to a fixed point on the chondrocranium during suction feeding in *Chiloscyllium plagiosum*. Peak times of selected buccal and hyoid variables are indicated. (A) Basihyal displacement (crystal 7 movement), lateral view as in Fig. 1. (B) Hyoid depression (vertical distance transduced by crystals 1, 4 and 7) and lateral compression (distance between crystals 5 and 6), anterior view.



of expansion in gape area contribute to an earlier onset of subambient pressure in the buccal and hyoid cavities.

#### Factors driving peak buccal and hyoid pressure

The velocity of gape and hyoid expansion appears to drive peak pressure in the buccal and hyoid cavities (Fig. 8). However, peak subambient pressure in the buccal and hyoid cavities is the result of complex interactions between gape and hyoid kinematics, hyoid lateral width decreasing as hyoid vertical depth increases, likely causing unsteady flow, which obscures the detection of a single predominant variable that is responsible for generating peak pressure. The time of peak buccal pressure also occurs simultaneously with peak area while the time of peak hyoid pressure coincides with peak velocity in the hyoid area. The faster the change in volume, the greater the subambient pressure generated. The lower the subambient pressures in the buccal and hyoid cavities, the greater the influx of water to draw prey into the mouth. This rapid mouth opening and expansion of the hyoid cavity also generates the sharp pressure drop in the buccal cavity that draws water and prey into the mouth of suction-feeding fishes (Liem, 1978; Liem, 1980; Lauder, 1980a; Lauder, 1980b; Lauder, 1983; Van Leeuwen and Muller, 1983; Muller and Osse, 1984; Lauder et al., 1986; Sanford and Wainwright, 2002; Svänback et al., 2002). Once peak gape is attained, water inflow and further subambient pressure decrease is limited. The same kinematic variables provide 60–63% of the variation in peak buccal and hyoid pressure. The velocity of gape and hyoid area expansion contribute the most to variation in peak buccal and hyoid pressure in *Chiloscyllium plagiosum*. A rapid

velocity of gape and hyoid expansion leads to a rapid increase in the change of volume in the buccal cavity resulting in lower subambient pressure. The buccal and hyoid regions generate the same mean magnitude of subambient pressure although hyoid pressure peaks prior to buccal pressure.

The peak rate of change in gape and hyoid area contributes more to the variation in peak pressure in *C. plagiosum* than the time of peak velocity or the time of peak percentage rate of change in area. Although the time of peak rate of change in gape area occurs earlier than the time of peak gape pressure, the time of peak rate of change in hyoid area occurs at the same time as peak hyoid pressure. The peak rate of percentage change in buccal area coincides with peak subambient buccal pressure in *M. salmoides* (Sanford and Wainwright, 2002), while peak gape area coincides with peak subambient buccal pressure in *C. plagiosum*. However, peak subambient pressure in the buccal cavity occurs much earlier than peak gape in teleosts, midway to peak gape in *M. salmoides* (Sanford and Wainwright, 2002; Higham et al., 2006) but 76% of the way to peak gape in *L. macrochirus* (Higham et al., 2006). It may be that the hyoid compression during the expansive phase in *C. plagiosum* delays the time to peak pressure as indicated by the inflection points in the pressure traces. Peak subambient pressure in the buccal and hyoid cavities of *C. plagiosum* (–5 to –99 kPa) is similar to that of other teleosts that are considered to be strong suction feeders, *Lepomis* species and *Hexagrammos decagrammus* (–30 to –71 kPa) (Lauder, 1980b; Nemeth, 1997; Higham et al., 2006). Other teleosts that rely more on bite or ram suction to capture prey generate relatively smaller peak subambient pressures (*M. salmoides*, *Cichlasoma severum*, *Cichla ocellaris*; –24.0

Table 3. Results from multiple stepwise linear regressions using time of onset of subambient buccal pressure (ms) as the dependent variable and kinematic variables as independent values during suction feeding in *C. plagiosum*

Regression model $P=0.0106$ , $r^2=0.7726$	Partial $F$ -statistic	Partial $P$ -value	Partial $r^2$	Standardized estimate
Gape area, onset (ms)	11.6281	0.0058	0.3901	0.53984
Gape area, peak (mm <sup>2</sup> )	8.5264	0.0139	0.0817	–0.83589
Gape area, peak velocity (mm <sup>2</sup> ms <sup>–1</sup> )	12.960	0.0042	0.0277	0.89191
Hyoid area, onset (ms)	2.3104	0.1560	0.0696	0.29801
Hyoid area, peak (ms)	2.1609	0.1693	0.0464	0.23418
Hyoid area, peak (mm <sup>2</sup> )	4.1616	0.0661	0.0491	–0.45463
Hyoid area, peak velocity (mm <sup>2</sup> ms <sup>–1</sup> )	4.0804	0.0682	0.0691	0.35365
Hyoid area, peak velocity (ms)	1.8769	0.1978	0.0388	0.25593

Table 4. Results from multiple stepwise linear regressions using peak subambient buccal pressure (kPa) as the dependent variable and kinematic variables as independent values during suction feeding in *C. plagiosum*

Regression model $P=0.0376$ , $r^2=0.5956$	Partial $F$ -statistic	Partial $P$ -value	Partial $r^2$	Standardized estimate
Gape area, onset (ms)	2.1904	0.1625	0.0682	–0.28555
Gape area, peak (mm <sup>2</sup> )	5.8564	0.0309	0.0390	0.68697
Gape area, peak velocity (mm <sup>2</sup> ms <sup>–1</sup> )	2.4649	0.1405	0.0842	–0.45249
Hyoid area, peak (ms)	2.250	0.1567	0.0652	–0.28123
Hyoid area, peak (mm <sup>2</sup> )	4.840	0.0464	0.1661	0.50308
Hyoid area, peak velocity (mm <sup>2</sup> ms <sup>–1</sup> )	6.1504	0.0278	0.1729	–0.52276

Table 5. Results from multiple stepwise linear regressions using time of onset of subambient hyoid pressure (ms) as the dependent variable and kinematic variables as independent values during suction feeding in *C. plagiosum*

Regression model $P=0.0078$ , $r^2=0.7425$	Partial $F$ -statistic	Partial $P$ -value	Partial $r^2$	Standardized estimate
Gape area, onset (ms)	10.4976	0.0071	0.2666	0.50658
Gape area, peak (ms)	4.410	0.0580	0.1570	0.35072
Gape area, peak (mm <sup>2</sup> )	7.290	0.0193	0.1168	–0.68908
Gape area, peak velocity (mm <sup>2</sup> ms <sup>–1</sup> )	8.9401	0.0112	0.0404	0.73660
Hyoid area, onset (ms)	3.2041	0.0982	0.0871	0.35926
Hyoid area, peak (mm <sup>2</sup> )	1.4641	0.2513	0.0312	–0.26826
Hyoid area, peak velocity (ms)	3.4596	0.0877	0.0434	0.34812

Table 6. Results from multiple stepwise linear regressions using peak subambient hyoid pressure (kPa) as the dependent variable and kinematic variables as independent values during suction feeding in *C. plagiosum*

Regression model $P=0.048$ , $r^2=0.6327$	Partial $F$ -statistic	Partial $P$ -value	Partial $r^2$	Standardized estimate
Gape area, onset (ms)	2.0736	0.1756	0.0954	-0.27696
Gape area, peak (mm <sup>2</sup> )	5.0176	0.0449	0.1712	0.64039
Gape area, peak velocity (mm <sup>2</sup> ms <sup>-1</sup> )	1.7161	0.2133	0.0529	-0.39566
Hyoid area, peak (ms)	3.0976	0.1034	0.1370	-0.32776
Hyoid area, peak (mm <sup>2</sup> )	3.9601	0.0699	0.0448	0.53596
Hyoid area, peak velocity (mm <sup>2</sup> ms <sup>-1</sup> )	3.8416	0.0735	0.1032	-0.41666
Hyoid area, peak velocity (ms)	1.7689	0.2094	0.0284	-0.29588

Table 7. Results from multiple stepwise linear regressions using time of onset of subambient pharyngeal pressure (ms) as the dependent variable and kinematic variables as independent values during suction feeding in *C. plagiosum*

Regression model $P\geq 0.0001$ , $r^2=0.9591$	Partial $F$ -statistic	Partial $P$ -value	Partial $r^2$	Standardized estimate
Gape area, onset (ms)	32.0356	0.0001	0.5754	1.28779
Gape area, peak (mm <sup>2</sup> )	4.7961	0.0509	0.0296	0.14211
Gape area, peak velocity (ms)	4.0000	0.0711	0.0550	-0.30489
Pharyngeal area, onset (ms)	3.2761	0.0974	0.0122	0.19974
Pharyngeal area, peak (ms)	7.7841	0.0175	0.0382	0.19683
Pharyngeal area, peak (mm <sup>2</sup> )	12.6025	0.0045	0.1561	-0.40750
Pharyngeal area, peak velocity (mm <sup>2</sup> ms <sup>-1</sup> )	6.9169	0.0236	0.0153	0.23674
Pharyngeal area, peak velocity (ms)	23.7169	0.0005	0.0774	-0.37676

Table 8. Results from multiple stepwise linear regressions using peak subambient pharyngeal pressure (kPa) as the dependent variable and kinematic variables as independent values during suction feeding in *C. plagiosum*

Regression model $P=0.0005$ , $r^2=0.8077$	Partial $F$ -statistic	Partial $P$ -value	Partial $r^2$	Standardized estimate
Gape area, peak (ms)	1.4641	0.2467	0.2162	0.27338
Gape area, peak (mm <sup>2</sup> )	16.000	0.0015	0.2276	0.52461
Gape area, peak velocity (mm <sup>2</sup> ms <sup>-1</sup> )	8.1225	0.0136	0.1019	-0.50575
Gape area, peak velocity (ms)	3.7636	0.0747	0.2120	-0.44312
Pharyngeal area, peak (ms)	1.9321	0.1893	0.0302	0.19196
Pharyngeal area, peak velocity (ms)	1.3456	0.266	0.0200	0.19898

to 15.6kPa) (Norton and Brainerd, 1993; Sanford and Wainwright, 2002; Svänback et al., 2002). As expected, the peak velocity of pressure change corresponds to the magnitude of peak subambient buccal pressure in these fish.

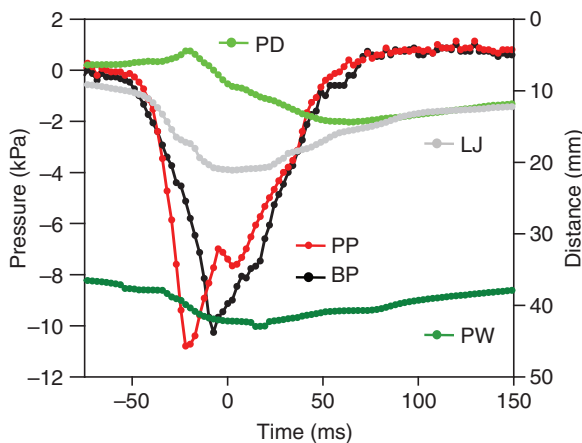


Fig. 5. Representative plot of buccal and pharyngeal kinematic and pressure variables during a suction-feeding event in *Chiloscyllium plagiosum*. Kinematic traces: PD, pharyngeal depression, dark green; PW, pharyngeal lateral expansion, light green; LJ, lower jaw depression, gray. Pressure traces: BP, buccal pressure, black; PP, pharyngeal pressure, red.

#### Factors driving the onset and peak pharyngeal pressure

Curiously, expansion of the branchial arches is not responsible for the initial drop in pressure in the pharynx in *Chiloscyllium plagiosum*. The onset of gape area is the predominant factor in contributing to the onset of, and variation in, subambient pressure in the pharynx (Fig. 8). The onset of pharyngeal pressure occurs simultaneously with the onset of increase in gape area, rather than

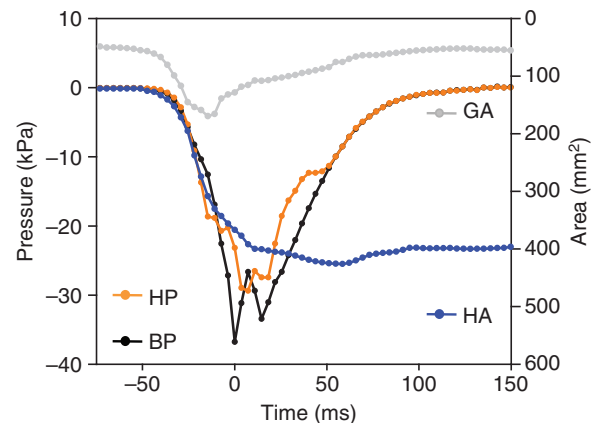


Fig. 6. Representative plot of buccal and hyoid variables during a suction-feeding event in *Chiloscyllium plagiosum*. Kinematic traces: GA, gape area, gray; HA, hyoid area, blue. Pressure traces: BP, buccal pressure, black; HP, hyoid pressure, orange.

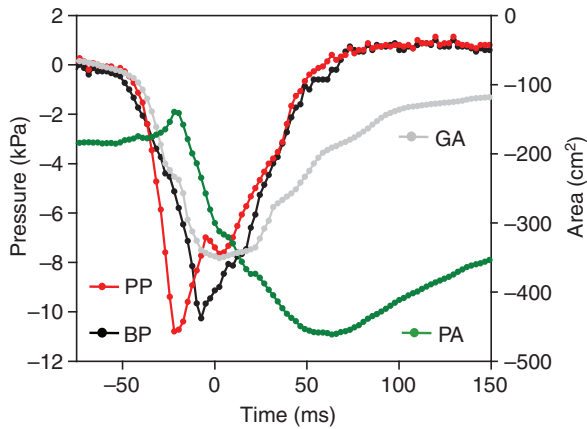


Fig. 7. Representative plot of buccal and pharyngeal variables during a suction-feeding event in *Chiloscyllium plagiosum*. Kinematic traces: GA, gape area, gray; PA, pharyngeal area, green. Pressure traces: BP, buccal pressure, black; PP, pharyngeal pressure, red.

with the onset of pharyngeal expansion. A possible explanation for this is that it appears that the conservation of flow momentum from the increasingly open gape through the hyoid to the pharynx and out of the fifth gill slit, which remains open throughout most of the feeding event, triggers the onset of subambient pressure in the pharyngeal cavity. Although the spiracle and first four gill slits are closed consistently during the expansive phase (Karch et al., 2007), leakage from the spiracle or fifth gill slit could also be responsible for a drop in pharyngeal pressure. A reversal in flow from the parabranial to the pharyngeal cavity occurs in *Lepomis* species and other elasmobranchs during feeding and ventilation and is accompanied by a positive pressure spike (Lauder, 1980b; Ferry-Graham, 1997; Ferry-Graham, 1999; Summers and Ferry-Graham, 2001). However, once the flow of water from the anterior to posterior expansion of the oropharyngeal cavities is established the momentum of water prevents flow reversal (Lauder, 1980a; Day et al., 2007). A positive pressure spike does not occur in the oropharyngeal cavity of *C. plagiosum* during prey capture; therefore a reversal of flow is not likely to be driving the onset of subambient pressure in the pharyngeal cavity unless it is masked by prevailing flow from the buccal cavity or parabranial cavities.

Several factors related to gape area appear to be driving peak subambient pressure in the pharyngeal cavity. Peak velocity and the time of peak velocity probably contribute the most to variation in peak pharyngeal pressure (Fig. 8). Again, the greater the velocity of expansion, the more water is moved at a greater velocity to drive peak subambient pressure in the pharynx. It is interesting that pharyngeal expansion is not the primary cause of peak pressure in this cavity. Pharyngeal area does not begin to increase until 3.5 ms prior to the time of peak pressure and expansion peaks 76 ms after peak pressure. Although the time of peak rate of change in pharyngeal area occurs earlier than peak pharyngeal pressure, the time of peak percentage rate of change in pharyngeal area occurs at peak pharyngeal pressure in *C. plagiosum*. Thus, the point at which the area of expansion in the pharynx reaches the greatest percentage is when pressure peaks, which occurs prior to peak gape. After this, flow from the buccal cavity must overwhelm the negative pressure generated by pharyngeal expansion and pressure slowly increases to ambient.

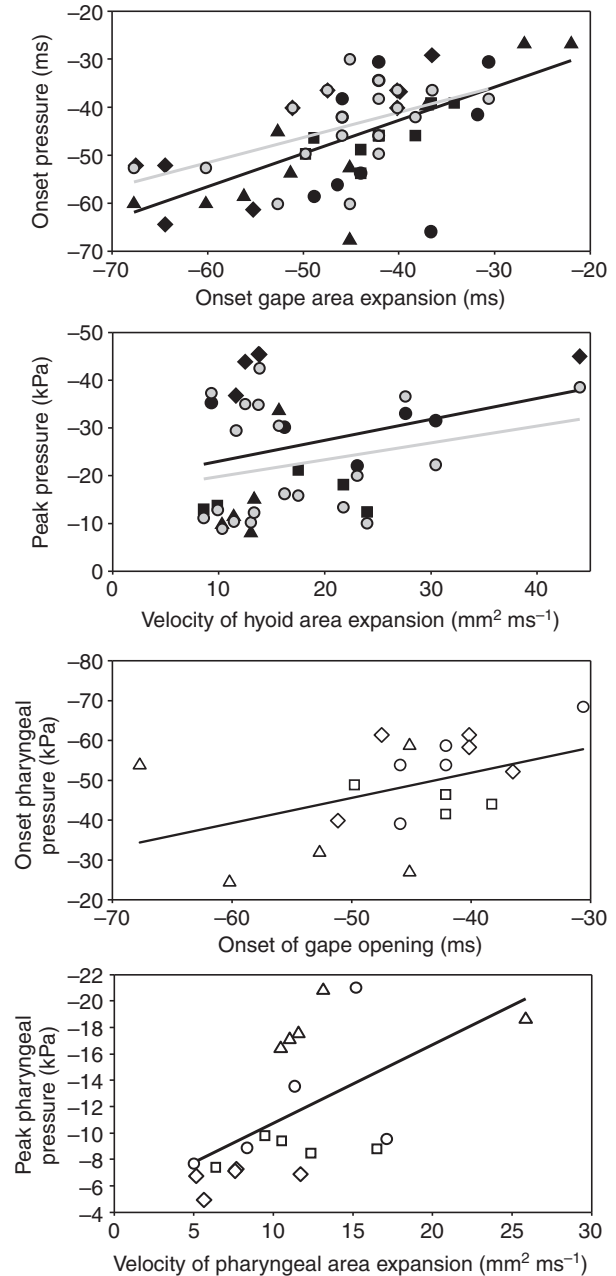


Fig. 8. Regression plots of the variables that contribute the most to the variation in onset and peak pressure in the oropharyngeal cavities. Top plot shows the time of onset of gape pressure [ $-15.203+(0.689 \times \text{time of onset of gape area increase})$ ,  $r^2=0.42$ ,  $P<0.001$ ] and the time of onset of hyoid pressure [ $-20.278+(0.521 \times \text{time of onset of gape area increase})$ ,  $r^2=0.27$ ,  $P=0.020$ ]. Second plot shows peak buccal pressure in kPa [ $-18.601-(0.439 \times \text{peak velocity of hyoid area expansion in } \text{mm}^2 \text{ ms}^{-1})$ ,  $r^2=0.086$ ,  $P=0.209$ ], and peak hyoid pressure in kPa [ $-16.245-(0.354 \times \text{peak velocity of hyoid area expansion in } \text{mm}^2 \text{ ms}^{-1})$ ,  $r^2=0.071$ ,  $P=0.257$ ]. Note that peak subambient pressure generation is the result of complex interactions of several variables with no one variable standing out (see Tables 4 and 6). Third plot shows the time of onset of pharyngeal pressure [ $-15.821+(0.725 \times \text{time of onset of gape area increase})$ ,  $r^2=0.58$ ,  $P<0.001$ ]. Bottom plot shows peak pharyngeal pressure in kPa [ $-4.777-(0.595 \times \text{peak velocity of pharyngeal area expansion in } \text{mm}^2 \text{ ms}^{-1})$ ,  $r^2=0.32$ ,  $P=0.009$ ]. Symbol shape indicates individual sharks; black, gray and white filled symbols indicate gape, hyoid and pharyngeal values, respectively.

### Evolutionary diversification of the suction mechanism in fishes

Peak pressure should and does occur early in the strike giving prey little chance to escape; however, peak pressure may also occur late in successful strikes, indicating that modulation of several kinematic events may be a factor. The relatively long chamber with different regions moving independently (compression with expansion) over a relatively long period of time, compared with teleosts, results in a complicated system from which a precise relationship between kinematics and pressure is difficult to extract. There is a wide range (8–60 ms) in the time to peak subambient pressure among teleost fishes as well as in *Chiloscyllium plagiosum* (23–77 ms), although the range is shifted 15–17 ms later in *C. plagiosum* compared with teleosts (Lauder, 1980b; Norton and Brainerd, 1993; Nemeth, 1997; Sanford and Wainwright, 2002). This later shift in peak pressure in *C. plagiosum* compared with teleosts is likely due to the delay caused by lateral compression of the hyoid. However, the coupled in-series linkage being more efficient in depressing the jaws and hyoid in teleosts or scaling effects cannot be ruled out.

The mechanism of suction feeding in *Chiloscyllium plagiosum* differs from that in actinopterygians primarily in movements of the hyoid arch due to morphological constraints (Wilga, 2008). In actinopterygians, volumetric expansion during suction feeding is due to dorsal elevation of the head, lateral expansion of the hyoid and suspensorium, upper jaw protrusion and ventral depression of the lower jaw and hyoid (Lauder and Shaffer, 1993; Sanford and Wainwright, 2002). In contrast, volumetric expansion by ventral depression of the lower jaw and ventral depression of the hyoid are the only elements that *C. plagiosum* have in common with actinopterygians. There is a stronger relationship between time to peak gape and pressure to buccal volume in *L. macrochirus* ( $r^2=0.95$ ) and *M. salmoides* ( $r^2=0.29$ ) (Higham et al., 2006) than in *C. plagiosum*. Perhaps the longer duration of suction generation in *C. plagiosum* compared with that in teleosts and lateral compression of the hyoid in *C. plagiosum* during the expansive phase, lacking in teleosts, allow more time and complexity of kinematic movements that may increase variation in the mechanism.

One of the most interesting and novel findings of this study is that *Chiloscyllium plagiosum* is able to generate large suction pressures while paradoxically compressing the hyoid cavity laterally simultaneous with expansion of the hyoid ventrally. Approximately a quarter of the way to peak hyoid depression, the distal ends of the hyomandibulae begin to adduct, which results in lateral compression of the hyoid cavity (Wilga, 2008). Suction inflow is momentarily stalled (see HP in Figs 3 and 6); when this happens a characteristic inflexion point occurs in the pressure profile and again when the hyomandibulae reach peak adduction (lateral compression) and begin to abduct back to the more lateral resting position. This stalling of pressure during suction feeding may be responsible for the delayed time to peak subambient pressure in *C. plagiosum* relative to actinopterygian fishes. More importantly, the two inflection points may hinder the ability to reveal clear kinematic correlates to the generation of pressure due to the complexity of lateral and ventral hyoid movement and the resulting pressure generated.

The hyostylic jaw suspension of elasmobranchs in conjunction with fewer degrees of freedom and the position of the hyomandibulae are responsible for lateral compression rather than expansion of the hyoid apparatus (Wilga, 2008). Sharks have a hyomandibula–ceratohyal–basihyal linkage, with laterally directed hyomandibulae, which constrains the distal ends to adduct when the basihyal is depressed. The methyostylic jaw suspension of actinopterygians contains an extra bone (interhyal) between the

vertically directed hyomandibulae and ceratohyal that increases freedom of movement (Schaeffer and Rosen, 1961; Wilga, 2002) and allows the hyomandibulae to abduct laterally even when the basihyal is depressed. Lateral compression simultaneous with ventral expansion of the hyoid in a strong suction-feeding shark species represents a significant departure from the suction mechanism in actinopterygian fishes, in which the hyoid cavity expands laterally and ventrally.

Cranial elevation and upper jaw protrusion are absent or slight in suction-feeding elasmobranchs, in direct contrast to actinopterygians and bite-feeding species (Wilga et al., 2007). Upper jaw protrusion is linked to lower jaw depression, therefore occurring simultaneously to increase volumetric expansion in actinopterygians (Lauder and Shaffer, 1993). Previous studies based on external kinematics have found that the onset of upper jaw protrusion occurs at or just after peak gape in suction-feeding shark species (Motta and Wilga, 2001; Motta, 2004). However, internal kinematics here reveals that the upper jaw begins to protrude shortly after the onset of lower jaw depression. Interestingly, considerable upper jaw protrusion contributes to buccal expansion in suction- and bite-feeding batoids similar to actinopterygians (Wilga and Motta, 1998b; Dean and Motta, 2004; Duquette and Wilga, 2007).

Rather than directly contributing to suction used to capture prey, pharyngeal expansion appears to act as a sink to receive the water influx during suction feeding. Several factors may limit pharyngeal expansion from effectively contributing suction for prey capture: the pharynx may be too distant from the buccal cavity, expansion and volume change occur too late, subambient pressure is too low, outflow through the opened fifth gill slit may preclude significant subambient pressure from developing. Studies on suction-feeding elasmobranch and actinopterygian fishes have focused on branchial and opercular expansion, respectively, rather than pharyngeal expansion due to the difficulties inherent in measuring the pharynx. Thus, the role of pharyngeal expansion during suction feeding has not yet been determined in actinopterygians.

Interestingly, the time of peak subambient pressure in the buccal, hyoid and pharyngeal cavities occurs in a posterior to anterior sequence. Pressure peaks in the pharyngeal cavity 44 ms, in the hyoid 52 ms, and in the buccal cavity 2 ms prior to peak area expansion in the corresponding region. Continued hyoid and pharyngeal expansion after peak gape probably functions simply to direct the influx of water and prey from the mouth into the pharynx, similar to the function of opercular expansion in teleost fishes (Lauder, 1985; Day et al., 2007). Expansion of the hyoid and pharyngeal cavities peaks simultaneously, supporting this premise. The slow return of pressure to ambient in the hyoid and pharynx is probably due to the flow of water keeping pace with expansion of the cavities and outflow through the fifth gill slits.

Aquatic turtles and salamanders expand the hyoid and pharyngeal cavities during aquatic ram and suction feeding in a similar process called compensatory suction (Lauder and Prendergast, 1992; Lemell and Weisgram, 1997; Summers et al., 1998). As the head is extended toward the prey, the hyoid and pharynx are expanded to collect the water flowing into the open mouth to prevent the forward movement of the head from pushing the prey away due to a bow wave (Lauder and Prendergast, 1992; Lemell and Weisgram, 1997; Summers et al., 1998; Ferry-Graham et al., 2003). *Chiloscyllium plagiosum* appears to use hyoid and pharyngeal expansion similarly to collect the water influx from the mouth, rather than contribute to the suction used to capture the prey. It appears that compensatory suction may be an integral part of suction feeding in some fishes and is not limited to unidirectional aquatic feeders lacking gill slits.

We thank J. Ramsay, J. Dolce, S. Gerry, L. Garcia and R. Iovino for assistance and anonymous reviewers who greatly improved the paper. This research was supported by the University of Rhode Island, Hofstra University, SeaWorld, Quaker Lane Bait and Tackle and a NSF IBN-0344126 grant to C.D.W.

## REFERENCES

- Carroll, A. M. and Wainwright, P. C.** (2006). Muscle function and power output during suction feeding in largemouth bass, *Micropterus salmoides*. *Comp. Biochem. Physiol. A* **143**, 389-399.
- Day, S. W., Higham, T. E. and Wainwright, P. C.** (2007). Time resolved measurements of the flow generated by suction feeding fish. *Exp. Fluids* **43**, 713-724.
- Dean, M. N. and Motta, P. J.** (2004). Feeding behavior and kinematics of the lesser electric ray, *Narcine brasiliensis*. *Zoology* **107**, 171-189.
- Dolce, J. and Wilga, C. D.** (2005). Gill slit kinematics in suction and ram ventilating sharks. *Integr. Comp. Biol.* **45**, 988.
- Duquette, D. C. and Wilga, C. D.** (2006). Mechanics of suction generation during feeding in little skates. *Integr. Comp. Biol.* **46**, e190.
- Ferry-Graham, L. A.** (1997). Feeding kinematics of juvenile swellsharks, *Cephaloscyllium ventriosum*. *J. Exp. Biol.* **200**, 1255-1269.
- Ferry-Graham, L. A.** (1999). Mechanics of respiration in swellsharks, *Cephaloscyllium ventriosum*. *J. Exp. Biol.* **202**, 1501-1510.
- Ferry-Graham, L. A. and Lauder, G. V.** (2001). Aquatic prey capture in ray finned fishes: a century of progress and new directions. *J. Morphol.* **248**, 99-119.
- Ferry-Graham, L. A., Wainwright, P. C. and Lauder, G. V.** (2003). Quantification of flow during suction feeding in bluegill sunfish. *Zoology* **106**, 159-168.
- Higham, T. E., Day, S. W. and Wainwright, P. C.** (2006). The pressures of suction feeding: the relation between buccal pressure and induced speed in centrarchid fishes. *J. Exp. Biol.* **209**, 3281-3287.
- Karch, A. P., Dolce, J. L. and Wilga, C. D.** (2006). Gill slit kinematics during ventilation and feeding in bamboo sharks. *Integr. Comp. Biol.* **46**, e214.
- Lauder, G. V.** (1980a). Evolution of the feeding mechanism in primitive actinopterygian fishes: a functional anatomical analysis of *Polypterus*, *Lepisosteus*, and *Amia*. *J. Morphol.* **163**, 283-317.
- Lauder, G. V.** (1980b). The suction feeding mechanism in sunfishes (*Lepomis*): an experimental analysis. *J. Exp. Biol.* **88**, 49-72.
- Lauder, G. V.** (1983). Prey capture hydrodynamics in fishes: experimental tests of two models. *J. Exp. Biol.* **104**, 1-13.
- Lauder, G. V.** (1984). Pressure and water flow patterns in the respiratory tract of the bass (*Micropterus salmoides*). *J. Exp. Biol.* **113**, 151-164.
- Lauder, G. V.** (1985). Aquatic feeding in lower vertebrates. In *Functional Vertebrate Morphology* (ed. D. M. B. M. Hildebrand, K. F. Liem and D. B. Wake), pp. 210-229. Cambridge: Harvard University Press.
- Lauder, G. V. and Prendergast, T.** (1992). Kinematics of aquatic prey capture in the snapping turtle *Chelydra serpentina*. *J. Exp. Biol.* **164**, 55-78.
- Lauder, G. V. and Reilly, S. M.** (1994). Amphibian feeding behavior: comparative biomechanics and evolution. *Adv. Comp. Environ. Physiol.* **18**, 163-195.
- Lauder, G. V. and Shaffer, H. B.** (1993). Design of feeding systems in aquatic vertebrates: major patterns and their evolutionary implications. In *The Skull: Functional and Evolutionary Mechanisms*, vol. 3 (ed. J. H. Hanken and B. K. Hall), pp. 113-149. Chicago: University of Chicago Press.
- Lauder, G. V., Wainwright, P. C. and Findeis, E.** (1986). Physiological mechanisms of aquatic prey capture in sunfishes: functional determinants of buccal pressure changes. *Comp. Biochem. Physiol.* **84A**, 729-734.
- Lemell, P. and Weisgram, J.** (1997). Feeding patterns of *Pelusios castaneus* (Chelonia: Pleurodira). *Neth. J. Zool.* **47**, 429-441.
- Liem, K.** (1978). Modulatory multiplicity in the functional repertoire of the feeding mechanism in cichlid fishes. *J. Morphol.* **58**, 323-360.
- Liem, K. F.** (1980). Acquisition of energy by teleosts: adaptive mechanisms and evolutionary patterns. In *Environmental Physiology of Fishes* (ed. M. A. Ali), pp. 299-334. New York: Plenum Publishing.
- Motta, P. J.** (2004). Prey capture behavior and feeding mechanics of elasmobranchs. In *Biology of Sharks and the Relatives* (ed. J. C. Carrier, J. A. Musick and M. R. Heithaus), pp. 139-164. Boca Raton: CRC Press.
- Motta, P. J. and Wilga, C. D.** (2001). Advances in the study of feeding mechanisms, mechanics, and behaviors of sharks. In *Biology and sensory biology of sharks: past, present and future studies*. *Environ. Biol. Fishes* **60**, 131-156.
- Muller, M. and Osse, J. W. M.** (1984). Hydrodynamics of suction feeding in fish. *Trans. Zool. Soc. Lond.* **37**, 51-135.
- Nauwelaerts, S., Wilga, C. D., Sanford, C. P. and Lauder, G. V.** (2007). Hydrodynamics of prey capture in sharks: effects of substrate. *J. R. Soc. Interface* **4**, 341-345.
- Nemeth, D. H.** (1997). Modulation of buccal pressure during prey capture in *Hexagrammos decagrammus* (Teleostei: Hexagrammidae). *J. Exp. Biol.* **200**, 2145-2154.
- Norton, S. F. and Brainerd, E. L.** (1993). Convergence in the feeding mechanics of ecomorphologically similar species in the centrarchidae and cichlidae. *J. Exp. Biol.* **176**, 11-29.
- Ramsay, J. B. and Wilga, C. D.** (2006). Hyoid mechanics and muscle function during feeding in white-spotted bamboo sharks, *Chiloscyllium plagiosum*. *Integr. Comp. Biol.* **46**, e140.
- Sanford, C. J. and Wainwright, P. C.** (2002). Use of sonomicrometry demonstrates the link between prey capture kinematics and suction pressure in largemouth bass. *J. Exp. Biol.* **205**, 3445-3457.
- Schaeffer, B. and Rosen, D. E.** (1961). Major adaptive levels in the evolution of the actinopterygian feeding mechanism. *Am. Zool.* **1**, 187-204.
- Summers, A. P. and Ferry-Graham, L. A.** (2001). Respiratory modes and mechanics of the hedgehog skate, *Leucoraja erinacea*: testing the continuous flow model. *J. Exp. Biol.* **204**, 1577-1587.
- Summers, A. P., Darouian, K. F., Richmond, A. M. and Brainerd, E. L.** (1998). Kinematics of aquatic and terrestrial prey capture in *Terrapene carolina*, with implications for the evolution of feeding in cryptodire turtles. *J. Exp. Zool.* **281**, 280-287.
- Svanbäck, R., Wainwright, P. C. and Ferry-Graham, L. A.** (2002). Linking cranial kinematics, buccal pressure and suction feeding performance in largemouth bass. *Physiol. Biochem. Zool.* **75**, 532-543.
- Van Leeuwen, J. L.** (1984). A quantitative study of flow in prey capture by rainbow trout, with general consideration of the actinopterygian feeding mechanism. *Trans. Zool. Soc. Lond.* **37**, 171-227.
- Van Leeuwen, J. L. and Muller, M.** (1983). The recording and interpretation of pressures in prey-sucking fish. *Neth. J. Zool.* **33**, 425-475.
- Van Wassenbergh, S., Herrel, A., Adriaens, D. and Aerts, P.** (2005). A test of mouth-opening and hyoid-depression mechanisms during prey capture in a catfish using high-speed cineradiography. *J. Exp. Biol.* **208**, 4627-4639.
- Westneat, M. W.** (2006). Skull biomechanics and suction feeding in fishes. In *Fish Biomechanics* (ed. R. E. Shadwick and G. V. Lauder), pp. 29-75. New York: Academic Press.
- Wilga, C. D.** (2002). A functional analysis of jaw suspension in elasmobranchs. *Biol. J. Linn. Soc. Lond.* **75**, 483-502.
- Wilga, C. D.** (2008). Evolutionary divergence in the feeding mechanism of fishes. *Acta Geol. Pol.* **58**, 113-120.
- Wilga, C. D. and Motta, P. J.** (1998a). Conservation and variation in the feeding mechanism of the spiny dogfish *Squalus acanthias*. *J. Exp. Biol.* **201**, 1345-1358.
- Wilga, C. D. and Motta, P. J.** (1998b). Feeding mechanism of the Atlantic guitarfish *Rhinobatos lentiginosus*: modulation of kinematic and motor activity. *J. Exp. Biol.* **201**, 3167-3184.
- Wilga, C. D. and Motta, P. J.** (2000). Durophagy in sharks: feeding mechanics of the hammerhead shark *Sphyrna tiburo*. *J. Exp. Biol.* **203**, 2781-2796.
- Wilga, C. D., Motta, P. J. and Sanford, C. P.** (2007). Evolution and ecology of feeding in elasmobranchs. *Integr. Comp. Biol.* **47**, 55-69.
- Wilga, C. D., Wainwright, P. C. and Motta, P. J.** (2000). Evolution of jaw depression mechanics in aquatic vertebrates: insights from Chondrichthyes. *Biol. J. Linn. Soc. Lond.* **71**, 165-185.